An Insight into a Novel Class of Self-Assembled Porphyrins: Geometric Structure, Electronic Structure, One- and Two-Photon Absorption Properties

Xin Zhou,[b] Ai-Min Ren,[b] and Ji-Kang Feng*[a]

Abstract: We have theoretically investigated a series of butadiyne-linked porphyrin derivatives that exhibit large two-photon absorption (TPA) cross sections in the visible-IR range. The electronic structure, one-photon absorption (OPA), and TPA properties have been studied in detail. We found that the introduction of a butadiyne linkage and the increase of the molecular dimensionality from monomer to dimer determine the OPA intensities of Q band and Soret band, respectively. A most important role for the enhancement of the TPA cross section is played by introducing a butadiyne bridge. The complementary coordination and the combination of the terminal free base and the core zinc porphyrin are also two effective factors for the enhancement of the TPA efficiency. The dimer with two porphyrins linked at meso-positions by a butadiyne linkage results in a maximum TPA cross section (79.35×10^{-48} cm^{4}s per photon). Our theoretical findings are consistent with the recent experimental observations. This series of porphyrin derivatives as promising TPA materials are the subject of further investigation.

Keywords: ab initio calculations · nonlinear optics · porphyrinoids · zinc · ZINDO-SOS

Introduction

Materials with large third-order nonlinear optical (NLO) polarizability have attracted much attention, because of potential utilities for photonic applications. High values of the real part result in nonlinear refraction, leading to scope for ultrafast all-optical signal processing,[1] while the imaginary part of the polarizability is responsible for two-photon absorption (TPA), which is useful for three-dimensional microfabrication,[2–5] ultra-high-density optical data storage,[6] biological imaging,[7] and the controlled release of biologically relevant species.[8] Various types of organic molecules have been investigated to obtain materials with large third-order nonlinearity γ. In general, it has been accepted that materials with π-conjugated systems terminated by donor and acceptor exhibit large γ values.[9–11] Porphyrins, notably porphyrin oligomers and polymers, are promising candidates as NLO materials in view not only of their large π-conjugated system, but also of versatile modifications of the structures and various possibilities of central metal ions as well to create porphyrins with ideal properties.[12–14]

Our recent interest focuses on the TPA properties of various materials. In order to enhance the TPA cross-section value, researchers are trying their best to establish the structure–property relationship. Albota et al.[15] synthesized and theoretically investigated a series of linear (dipolar and quadrupolar) molecules with different D/A combinations attached to a π center (D = donor, A = acceptor). They pointed out that conjugation length, D/A strength, and molecular symmetry are important factors responsible for the increase of TPA cross sections. Kim et al.[16] found that the TPA cross sections of chromophores with dithienothiophene as a π center was nearly one order of magnitude larger than those with fluorene as a π center, indicating that the π center should play an important role in the TPA response of materials. Most recently, researchers have turned their attention to design and synthesize multibranched (or octupolar) and dendritic molecules to further increase TPA cross section.[17–21] In comparison with the dipolar molecules, the major advantages of octupolar compounds are greater likelihood of producing crystals with noncentrosymmetric packing (donor–acceptor molecules have a propensity to align in an antiparallel fashion which oppose dipoles), and improved nonlinearity–transparency trade-off (due to a decreased conjugation pathway).

However, only a limited number of reports of the TPA cross sections for porphyrins are available. Wen et al.[22] measured the TPA cross sections of metal–tetrakis(3,4,5-tri-

[a] Prof. J.-K. Feng
State Key Laboratory of Theoretical and Computational Chemistry
Institute of Theoretical Chemistry, and College of Chemistry
Jilin University, Changchun 130023 (China)
Fax: (+86) 431-894-5942
E-mail: jikangf@yahoo.com

[b] Dr. X. Zhou, Prof. A.-M. Ren
State Key Laboratory of Theoretical and Computational Chemistry
Institute of Theoretical Chemistry
Jilin University, Changchun 130023 (China)

 DOI: 10.1002/chem.200400251

methoxyphenyl)porphyrin, including chlorogallium(III), chloroindium(III), chlorothallium(III), tin(II), and lead(II) as central metal ions, with the linear polarized nanosecond laser pulses at different wavelengths by Z-scan. The observed TPA cross sections are in the range of 25–114 × 10^{-50} cm^4 s per photon. Rebane and co-workers[23] obtained the absolute TPA cross sections for a series of porphyrins and tetrazaporphyrins with pulses of 100 fs duration in two ranges of laser wavelengths, from 1000 to 1500 and from 700 to 800 nm. They found that the TPA cross section in the Soret transition region is larger than that in the Q transition region by one order of magnitude. Screen et al.[24] reported a double-strand conjugated porphyrin polymer linked by butadiyne bonds exhibiting large TPA cross-section values of 5 × 10^{-46} cm^4 s per photon), which were measured by a degenerate four-wave mixing method with a picosecond pulse laser. Most recently, Rebane and co-workers[25] observed a 400-fold enhancement of TPA in a conjugated porphyrin dimer, relative to its related monomer at 780 nm. In contrast to the experimental investigations, there are few theoretical reports on the TPA properties of porphyrins. Birge et al.[26] studied the TPA properties of free-base porphyrin, free-base porphyrin dianion, and the 2,4-substituted diformal and divinyl analogues of these molecules using a semiempirical SCF-MO formalism. They showed that a number of the two-photon allowed states in the Soret region are predicted to have TPA exceeding 100×10^{-50} cm^4 s per photon. Quite recently, our group[27] studied a class of porphyrin-derived monomers and dimers. The TPA cross-section values of dimer porphyrins were found to be 25–100 times larger than those of monomers.

In this work, we have theoretically investigated the equilibrium geometries, electronic structures, one-photon absorption (OPA), and TPA properties of self-assembled porphyrin monomers and dimers, which were recently synthesized by Ogawa and co-workers.[28]

Computational Methods

The TPA process corresponds to simultaneous absorption of two photons. The TPA efficiency of an organic molecule, at optical frequency, can be characterized by the TPA cross section. It can be directly related to the imaginary part of the second hyperpolarizability by Equation (1):[29,30]

$$\delta(\omega) = \frac{3(\hbar\omega)^2}{2n^2c^2\varepsilon_0\hbar} L^4 \mathrm{Im}[\gamma(-\omega;\omega,-\omega,\omega)] \quad (1)$$

in which $\gamma(-\omega;\omega,-\omega,\omega)$ is the orientational average of the third-order molecular polarizability, $\hbar\omega$ the energy of the incoming photons, ε_0 the vacuum electric permittivity, n deotes the refractive index of the medium, and L corresponds to the local-field factor. In the calculations presented here, these last two quantities are set to 1 (isolated molecule in vacuum).

The sum-over-states (SOS) expression to evaluate the components of the second hyperpolarizability $\gamma_{\alpha\beta\gamma\delta}$ can be deduced by using perturbation theory and density matrix method. By considering a power expansion of the energy with respect to the applied field, the $\gamma_{\alpha\beta\gamma\delta}$ Cartesian components are given by Equation (2):[31,32]

$$\gamma_{\alpha\beta\gamma\delta}(-\omega_\sigma;\omega_1,\omega_2,\omega_3) = \hbar^{-3}\sum P_{1,2,3}\left(\sum_K{}'\sum_L{}'\sum_M{}'\left(\frac{\langle 0|\mu_\alpha|K\rangle\langle K|\overline{\mu_\beta}|L\rangle\langle L|\overline{\mu_\gamma}M\rangle\langle M|\mu_\delta|0\rangle}{(\omega_K - i\Gamma_K - \omega_\sigma)(\omega_L - i\Gamma_L - \omega_2 - \omega_3)(\omega_M - i\Gamma_M - \omega_3)} + \frac{\langle 0|\mu_\beta|K\rangle\langle K|\overline{\mu_\alpha}|L\rangle\langle L|\overline{\mu_\gamma}|M\rangle\langle M|\mu_\delta|0\rangle}{(\omega_K + i\Gamma_K + \omega_1)(\omega_L - i\Gamma_L - \omega_2 - \omega_3)(\omega_M - i\Gamma_M - \omega_3)}\right.\right.$$

$$+\frac{\langle 0|\mu_\beta|K\rangle\langle K|\overline{\mu_\gamma}|L\rangle\langle L|\overline{\mu_\alpha}|M\rangle\langle M|\mu_\delta|0\rangle}{(\omega_K + i\Gamma_K + \omega_1)(\omega_L + i\Gamma_L + \omega_1 + \omega_2)(\omega_M - i\Gamma_M - \omega_3)} + \left.\frac{\langle 0|\mu_\beta|K\rangle\langle K|\overline{\mu_\gamma}|L\rangle\langle L|\overline{\mu_\delta}|M\rangle\langle M|\mu_\alpha|0\rangle}{(\omega_K + i\Gamma_K + \omega_1)(\omega_L + i\Gamma_L + \omega_1 + \omega_2)(\omega_M + i\Gamma_M + \omega_\sigma)}\right) - \sum_K{}'\sum_L{}'\left(\frac{\langle 0|\mu_\alpha|K\rangle\langle K|\mu_\beta|0\rangle\langle 0|\mu_\gamma|L\rangle\langle L|\mu_\delta|0\rangle}{(\omega_K - i\Gamma_K - \omega_\sigma)(\omega_K - i\Gamma_K - \omega_1)(\omega_L - i\Gamma_L - \omega_3)}\right.$$

$$\left.\left.+\frac{\langle 0|\mu_\alpha|K\rangle\langle K|\mu_\beta|0\rangle\langle 0|\mu_\gamma|L\rangle\langle L|\mu_\delta|0\rangle}{(\omega_K - i\Gamma_K - \omega_1)(\omega_L + i\Gamma_L + \omega_2)(\omega_L - i\Gamma_L - \omega_3)} + \frac{\langle 0|\mu_\beta|K\rangle\langle K|\mu_\alpha|0\rangle\langle 0|\mu_\gamma|L\rangle\langle L|\mu_\delta|0\rangle}{(\omega_K + i\Gamma_K + \omega_1)(\omega_K + i\Gamma_K + \omega_\sigma)(\omega_L + i\Gamma_L + \omega_2)} + \frac{\langle 0|\mu_\beta|K\rangle\langle K|\mu_\alpha|0\rangle\langle 0|\mu_\gamma|L\rangle\langle L|\mu_\delta|0\rangle}{(\omega_K + i\Gamma_K + \omega_1)(\omega_L + i\Gamma_L + \omega_2)(\omega_L - i\Gamma_L - \omega_3)}\right)\right) \quad (2)$$

In this formula α, β, γ, and δ refer to the molecular axes; ω_1, ω_2, and ω_3 are optical frequencies and $\omega_\alpha = \omega_1 + \omega + {}_2\omega_3$ is the polarization response frequency; $\Sigma P_{1,2,3}$ indicates a sum over the terms obtained by the six permutations of the pairs (ω_1/μ_β),(ω_2/μ_γ), and (ω_3/μ_δ); $|K\rangle$ is an electronic wavefunction with energy $\hbar\omega_K$ relative to the ground electronic state; μ_α is the αth ($=x, y, z$) component of the dipole operator, $\langle K|\mu_\alpha|L\rangle = \langle K|\mu_\alpha|L\rangle - \langle 0|\mu_\alpha|0\rangle$; the primes on the summation over the electronic states indicate exclusion of the ground state. Γ_K is the damping factor of excited state K, in the present work, all damping factors Γ_K are set to 0.16 eV; this choice of damping factor is found to be reasonable on the basis of the comparison between the theoretically calculated TPA spectra and Z-scan TPA spectra.

Results and Discussion

Geometry optimization and electronic structure: The molecular structures are shown below. The *meso*-(*N*-methyl)imidazolylporphyrinatozinc compound **1M** quantitatively affords a dimer of a slipped cofacial orientation **1D** by the complementary coordination of an imidazolyl group to the zinc(II) center. In compound **2M**, imidazolylporphyrinatozinc and free-base porphyrin are directly linked at *meso*-positions. The dimer of **2M** is the self-assembly product **2D**. To expand the π-conjugation between two porphyrin units, two imidazolylporphyrins are connected by a butadiyne unit to allow a coplanar orientation in chromophore **3M** and the dimer of **3M** (i.e., **3D**). In order to study the effects of the complementary coordination of the metal zinc(II) atom and the introduction of acceptor groups on the OPA and TPA properties, analogues of **3M**, that is, **4**, **5** and **6** were investigated. The geometric structures are optimized using the Gaussian 98 program with 6-31G basis set at the hybrid three-parameter Becke exchange functional and Lee-Yang-Parr correlation functional (B3LYP) level. The optimized results show that the compounds **1D**, **2D**, **3D**, **4**, and **6** pos-

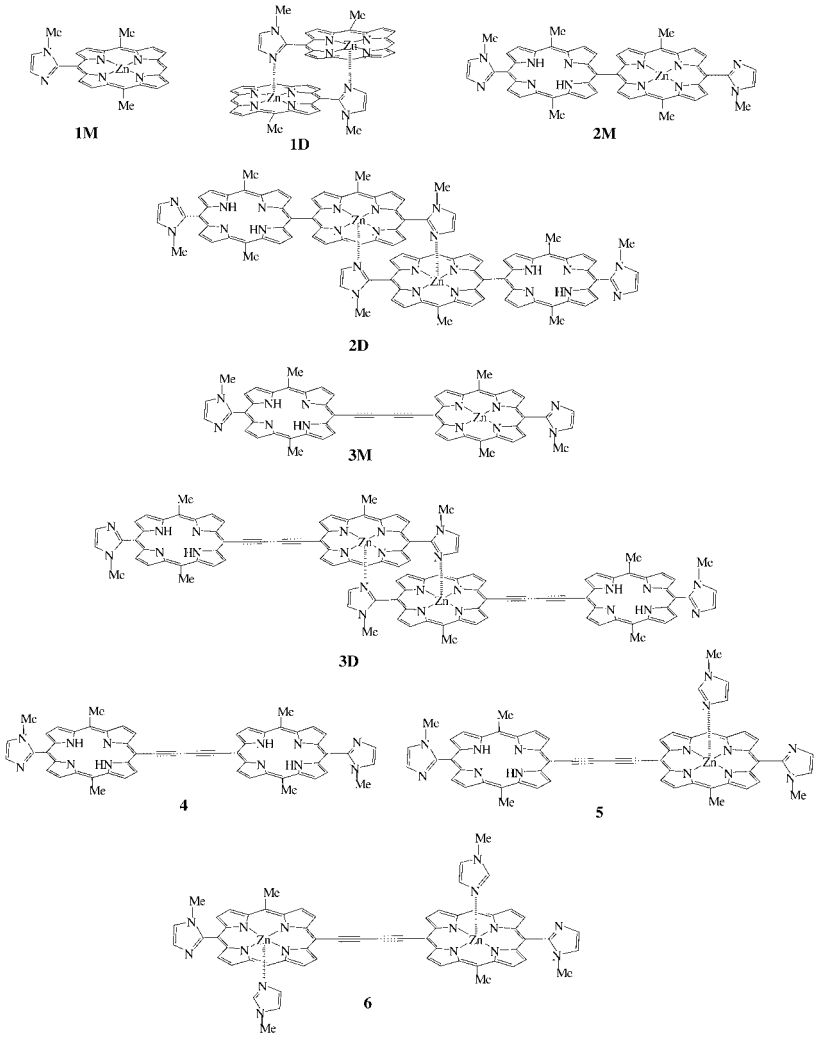

sess C_i symmetry and there are no symmetric constraints on other molecules. In the case of monomers **1M**, **2M**, **3M**, and molecule **4**, the porphyrin macrocycles are practically planar. The Zn–N bond lengths in **1M**, **2M**, and **3M** are on average 2.046 Å. In compounds **2M** and **2D**, the dihedral angles between two porphyrins are 87.5°and 81.8°, respectively, which is consistent with the experimentally almost orthogonal structure .[28] For compounds with the complementary coordination of the imidazolyl to zinc(II) such as **1D**, **2D**, **3D**, **5**, and **6**, the imidazolyl group is almost perpendicular to the porphyrin plane (85.7°). As for dimers **1D**, **2D**, and **3D**, the average Zn–N bond length in porphyrin rings is 2.103 Å, which is longer than that in monomers (2.046 Å). The above results are due to the fact that the coordination between zinc(II) atom and imidaxolyl makes the zinc(II) atom close to imidizolyl ring and out of the porphyrin plane, so that the Zn–N bonds are lengthened and the planar porphyrins are distorted. The distances between the zinc(II) atom and N atom in imidiazolyl rings are 2.142 Å (for **1D**), 2.147 Å (for **2D**), 2.138 Å (for **3D**), 2.121 Å (for **5**) and 2.131 Å (for **6**). In **1D**, two porphyrin rings are separated at a distance of 3.578 Å and the Zn–Zn distance is 6.128 Å; these values are close to the interplanar distance of 3.23 Å and a metal–metal distance of 6.13 Å, respectively, determined by X-ray crystallography.[33] The average dihedral angle between an imidazolyl ring without coordination and the porphyrinatozinc plane of molecules is 64.4°, which is larger than that between the free-base porphyrin and imidiazolyl-59.7°.

The energies of some frontier orbitals and the shapes of the two highest occupied molecular orbitals (HOMO) and two lowest unoccupied molecular orbitals (LUMO) obtained by B3LYP6–31G method, are shown in Figures 1 and 2, respectively. As seen in Figure 1, the energy of LUMO decreases with the increase in the conjugation length in the order **1M** (−2.24 eV), **2M** (−2.37 eV), **3M** (−2.77 eV) and **1D** (−1.90 eV), **2D** (−2.25 eV), **3D** (−2.67 eV). The LUMO+1 levels exhibit the same trend (−2.15 eV, −2.29 eV, −2.35 eV and −1.86 eV, −2.24 eV, −2.64 eV). However, the energy of HOMO is little affected by the extension of conjugation length. The energy gap between HOMO and LUMO

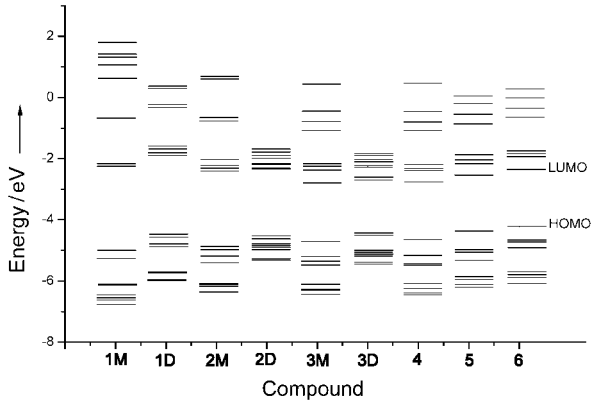

Figure 1. Molecular orbital diagrams summarizing results predicted by the B3LYP6-31G method.

decreases with the increase of the conjugation length (2.79 eV (**1M**) > 2.57 eV (**2M**) > 1.96 eV (**3M**) and 2.61 eV (**1D**) > 2.34 eV (**2D**) > 1.80 eV (**3D**)). As shown in Figure 1, the energy gaps between HOMO and LUMO of dimers are smaller that that of the corresponding monomers (2.79 eV (**1M**) > 2.61 eV (**1D**), 2.57 eV (**2M**) > 2.34 eV (**2D**), 1.96 eV (**3M**) > 1.83 eV (**3D**)). Comparing **3M** and

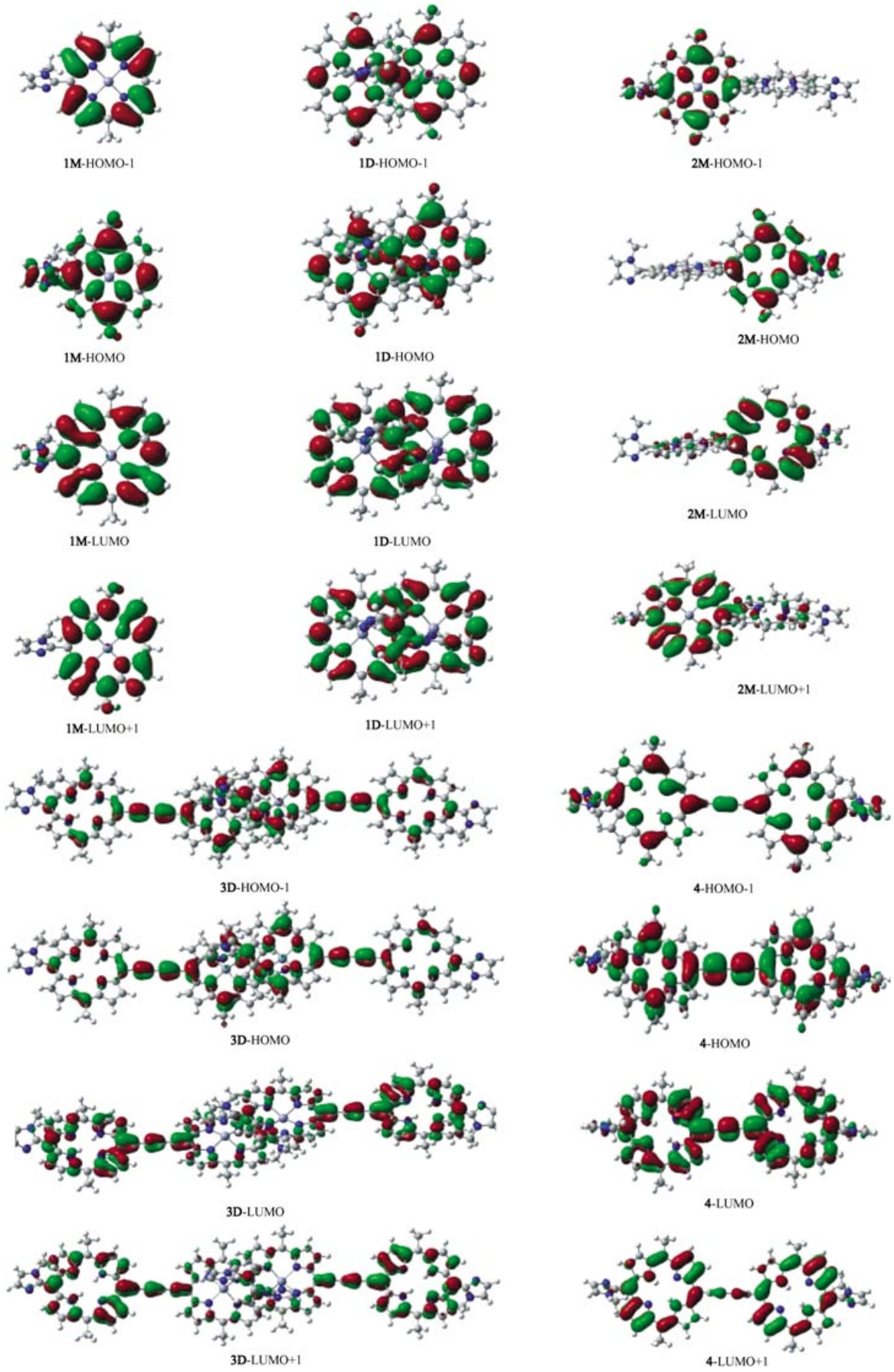

Figure 2. Two highest occupied and two lowest unoccupied molecular orbitals.

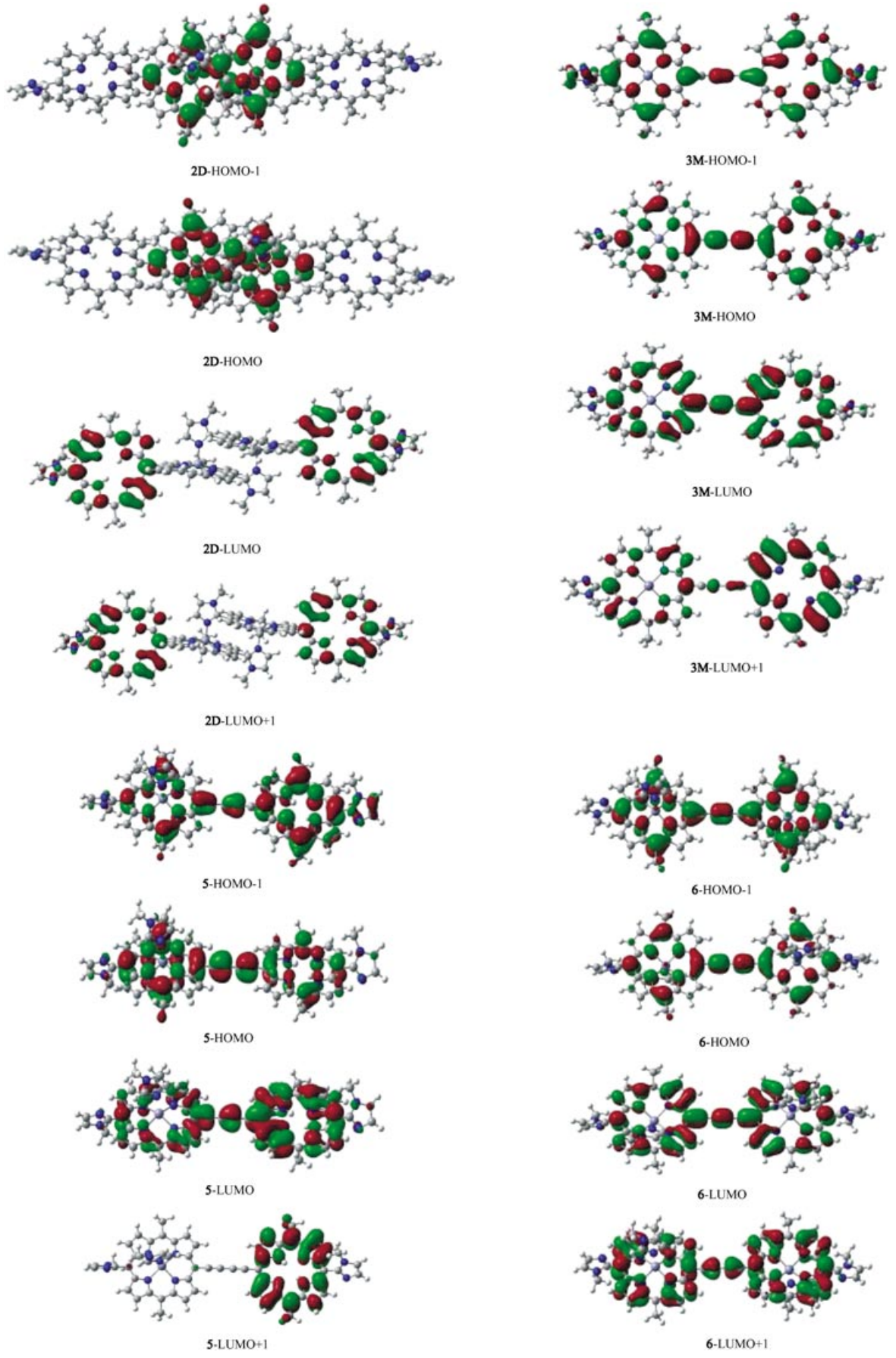

Fig. 2 (continued).

its analogues **4**, **5** and **6**, one can find that **3M** and **4** show very similar electron structures, and there are some differences between the distributions of orbital energy for **3M** and **5**. These results show that the complementary coordination of the metal zinc(II) atom has some effect on the electronic structure of molecules. With the increase of zinc(II) atom from **4** to **5** and to **6**, the HOMO and LUMO become more unstable (LUMO: −2.80 eV (**4**)→−2.58 eV (**5**) →-2.35 eV (**6**), HOMO: −4.47 eV(**4**)→-4.43 eV (**5**)→-4.24 eV (**6**)). However, the energy gap between HOMO and LUMO changes little. The standard interpretation of the origin of the Q and B bands in the electronic absorption spectra of porphyrins is based on the four-orbital model of Goutermans,[34,35] which assumes that the HOMO and HOMO−1 are almost degenerate in energy and well separated from the other levels; a similar assumption is made for the LUMO and LUMO+1.

Evidently, as can be seen from Figure 1, the four-orbital model approximately describes **1M**, because the other frontier orbitals are separated by a comparatively large energy gap between two highest HOMOs and two lowest LUMOs. However, for other molecules the four-orbital model is not applicable. This due to the fact that either the two highest HOMOs and two lowest LUMOs are not quasi-degenerate for **3M**, **4**, **5**, **6**, or the energy gap between the degenerate HOMOs or LUMOs and other orbitals in **1D**, **2M**, **2D**, **3D** is smaller than 1 eV, and the configuration interaction involving orbitals close in energy to two HOMOs and LUMOs for all molecules is strong. The reason for these results is that owing to the change in orbital symmetry, the presence of other orbitals in the vicinity of HOMOs and LUMOs does not automatically guarantee strong configuration interaction.

Examining Figure 2, we find for **1D**, **2D**, and **3D**, two HOMOs and two LUMOs exhibit the nearly same shapes due to their degeneracy. In the case of **1M**, the coefficients of two HOMOs on porphyrin are hardly changed in comparison with that of zinc porphyrin[36] and the contribution of the imidazolyl ring is added to the HOMO. However, the characters of LUMO and LUMO+1 change a lot. Comparing LUMO+1 of **1M** with that of zinc porphyrin, the contribution of the *meso*-carbon atoms parallel with the imidazolyl disappear and the contributions of pyrrole nitrogens are added. The LUMO coefficients are mostly localized on the whole porphyrin ring, except for the Zn atom. These results indicate that the addition of imidazolyl ring has an effect on the LUMOs of molecule. The two degenerate HOMOs and two degenerate LUMOs of **1D** show the same character as that of the HOMO and LUMO of **1M**. As for **2M**, since two porphyrin rings are nearly perpendicular to each other, the intramolecular conjugation is broken and the population of electron cloud of HOMOs and LUMOs focuses on one porphyrin ring. The same phenomenon appears in **2D**. The introduction of a butadiyne bridge results in the planarity of the whole molecule **3M** and **3D**. As in the case of **3D**, the two degenerate HOMOs receive a major contribution from the *meso*-carbon atoms, the pyrrole nitrogen atoms in zinc porphyrin, and the butadiyne bridge, while the degenerate LUMOs coefficients are largely localized on the α- and β-carbon atoms of the free-base porphyrin and the butadiyne linkage. It is known that the electronic transition from HOMOs to LUMOs have important contributions to the Q and B bands of porphyrins. In reference [37], the authors investigated the TPA properties of a series of dipole and quadrupole molecules, and drew the conclusion that the charge transfer is effective in enhancing the two-photon absorptivity irrespective of the direction of the transfer (from the ends to the center of the molecule or from the center to the ends). So for **3D**, the charge transfer from the inner zinc porphyrin to the terminal free base (shown in Figure 2) will result in the evident enhancement of TPA cross section. Analyzing the frontier orbitals of **4**, **5** and **6**, we find that in the cases of centrosymmetric **4** and **6**, HOMOs and LUMOs equally localized on two porphyrins and there is no evident charge transfer. However, for **5**, the intramolecular charge-transfer is clearly seen. From the HOMOs to LUMOs, the contribution from the zinc porphyrin ring to the molecular orbital becomes less and less. In LUMO+1, the coefficients are completely localized on the terminal free-base porphyrin. It means that from HOMO−1 to LUMO+1, the charge is completely transferred from zinc porphyrin ring to free-base porphyrin. From these results, we can predict that compound **5** will exhibit larger TPA cross section than that of **4** and **6**.

One-photon absorption: The OPA properties of all molecules have been calculated by using the ZINDO program on the basis of geometric structures optimized by B3LYP6-31G level. Figure 3 displays the OPA spectra of dimers **2D** and **3D** and the corresponding experimental data.[28] In the experimental report,[28] the C_7H_{15} groups are at the *meso*-positions of porphyrin ring. However, in our calculation, C_7H_{15} groups are replaced by methyl groups in order to save the calculating time. The active Q and Soret bands with large OPA intensities and the corresponding oscillator strength are listed in Table 1 and some experimental data are given in parentheses. As shown in Table 1 and Figure 3, the calculated values are in good agreements with the experimental observations. Weak Q band and intense Soret bands are found in the regions of about 580–800 and 300–500 nm. Table 1 shows clearly that there is a splitting of the Soret bands for every compound. The magnitude of the splitting of the Soret bands increases with the increase of the conjugation length (1.2 nm (**1M**) < 64.0 nm (**2M**) < 86.2 nm (**3M**), 30.0 nm (**1D**) < 42.5 nm(**2D**) < 91.9 nm(**3D**)). In the case of molecules **4**, **5**, and **6**, with the replacement of zinc porphyrin with free-base porphyrin, the splitting slightly increases from 83.3 nm for **4** to 90.7 nm for **5** and to 93.2 nm for **6**. The large splitting of the Soret bands that appeared in the calculated OPA spectra of molecules around 300–500 nm was also observed experimentally by Ogawa et al.[38]

The results in Table 1 demonstrate that the expansion of the π conjugation between porphyrin units by introducing a butadiyne linkage and the increase of molecular dimensionality from monomers to dimers play different roles in the enhancement of OPA intensities of the studied compounds. For the Q-band absorption of molecules, the introduction of a butadiyne linkage is the most important parameter for de-

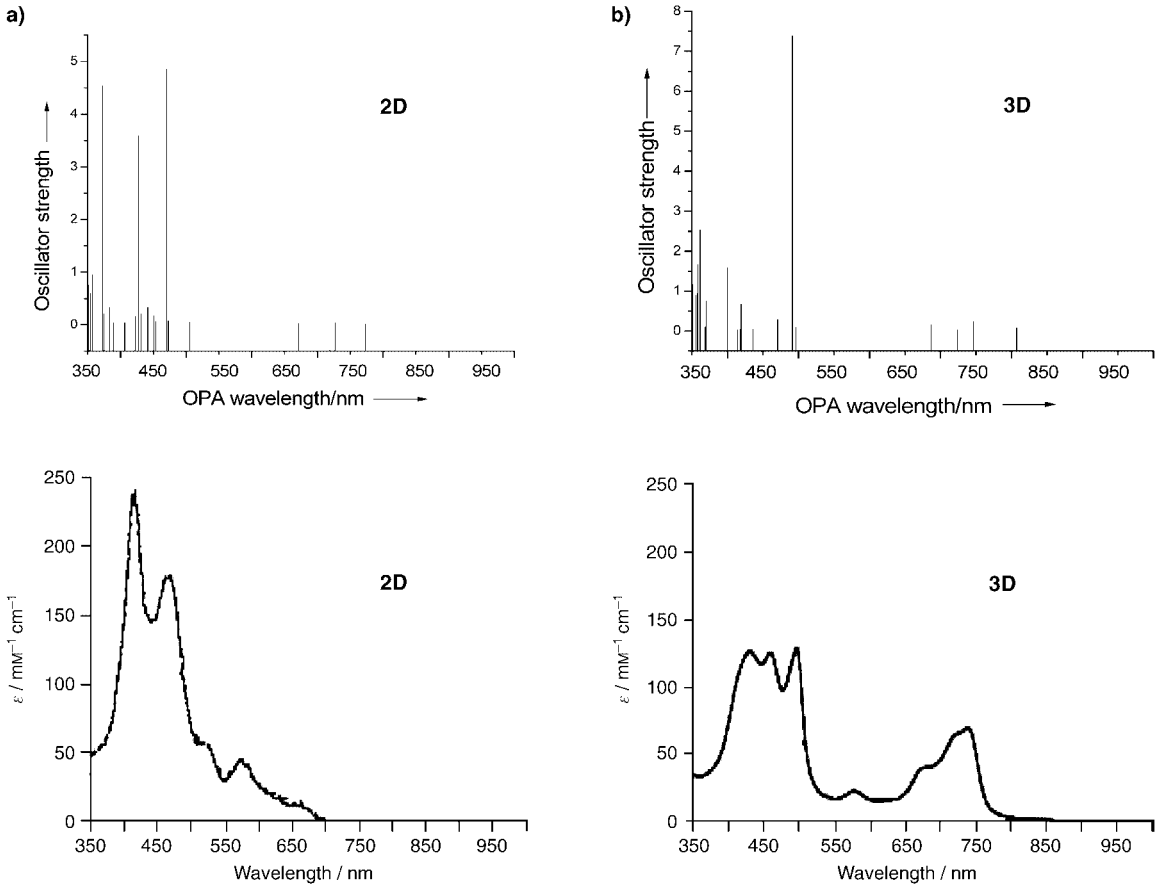

Figure 3. Theoretical and experimental one-photon absorption spectra of a) **2D** and b) **3D** (figures at the top are the theoretical data in this work and figures at the bottom are the experimental data in reference [28]).

termining the OPA intensities. Compounds **1M** and **1D** have quite small oscillator strengths of the Q band, probably due to their small size. However, porphyrins linked directly at *meso*-positions in **2M** and **2D** do not give rise to an increase of oscillator strength; this comes from the fact that almost orthogonal porphyrins have almost no effect on the conjugation length. A relatively significant change occurs when butadiyne linkages are introduced in **3M** and **3D**. The oscillator strength in the Q band of **3M** is found to be 0.14, which is seven times that of **1M** and 23 times that of **2M**. Such conjugation dependence works well for dimers **1D**, **2D**, and **3D**. Molecules **4**, **5**, and **6** also have comparatively strong Q-band absorptions owing to the presence of the butadiyne moiety. In **3D**, **4**, **5**, and **6**, the porphyrin rings interact though the linking of butadiyne moiety, and the conjugation length in the molecules is extended; consequently the OPA intensity of Q band is strengthened. The increase of the molecular dimensionality from monomers to dimer analogues plays a significant role in the oscillator strength of the B-band absorption. The oscillator strength of **1D** is found to be 7.23, which is five times that of **1M**. From **2M** to **2D** and **2M** to **3D**, more than twofold enhancements of the OPA intensity are observed. The results show that the linkage of imidazolyl groups strengthens coupling effects between two monomers and so enhances the OPA strength of Soret band.

Two-photon absorption: In general, it is difficult to assess the molecular TPA efficiency among different materials from a direct comparison of their TPA cross sections. This is either because the measurements by different groups were not always carried out under comparable experimental conditions or because some of the materials were only measured using one single wavelength.[39,40] However, theoretical simulations should be able to provide fair information appropriate for comparison. In the present study, we have compiled a program to calculate the third-order optical susceptibility and the TPA cross section according to Equations (1) and (2). The TPA spectra of molecules in the incident wavelength range of 550–1300 nm are shown in Figure 4. It is observed that there are multiple peaks in some TPA spectra. The calculated main peaks in the spectra and the corresponding TPA cross section values are summarized in Table 1. The data in parentheses were obtained by an open-aperture Z-scan method at wavelengths from 817 nm to 1282 nm by using a femtosecond optical parametric amplifier.[28] As shown in Table 1, the calculated TPA parameters are consistent with the experimental results. Normally, the TPA process should happen in the region without OPA. Furthermore, in many applications of two-photon features, molecules with large TPA cross sections are required in a range of fundamental excitation wavelengths, that is, 600–1200 nm. Therefore, we only discuss the maximum TPA

Table 1. One- and two-photon absorption properties of the compounds described.[a]

	$\lambda_{max}^{(1)}$ [nm]	f	$\lambda_{max}^{(2)}$ [nm]	δ_{max} [10^{-48} cm^{4}s per photon]
1M	626.1	0.01339	**663.0**	**0.69**
	621.4	0.01309		
	351.0	0.92494		
	349.8	0.79276		
1D	583.7	0.02986	**685.0**	**1.82**
	581.3	0.01069		
	338.2	4.17083		
	308.2	3.06374		
2M	655.2	0.00130	**704.4**	**1.45**
	589.0	0.00563	593.2	1.45
	386.5	1.48526		
	322.5	2.05338		
2D	772.6	0.01116	**905.0**(964)[28]	**3.72**(3.7)[28]
	726.8	0.03302		
	470.0(~472)[28]	4.86186		
	427.5(~428)[28]	3.59187		
3M	667.5	0.02195	**729.3**	**20.51**
	588.6	0.12768	632.5	30.66
	435.1	2.41712		
	348.9	0.91148		
3D	807.1	0.07990	**849.2**(887)[28]	**79.35**(76)[28]
	746.3	0.22830		
	491.5(~499)[28]	7.38643		
	399.6	1.58090		
4	683.1	0.03311	**832.1**(873)[28]	**10.26**(10)[28]
	585.0	0.21253	733.6	19.18
	443.4	2.03652	652.5	32.89
	360.1	1.42447		
5	670.4	0.03713	**770.1**	**25.61**
	624.2	0.11288	652.5	23.07
	451.5	2.20240		
	360.8	1.22737		
6	634.4	0.15790	**779.8**	**18.76**
	619.7	0.01053	659.4	30.94
	442.9	3.26720		
	349.7	0.89152		

[a] The experimental results taken from reference [28] are shown in parentheses.

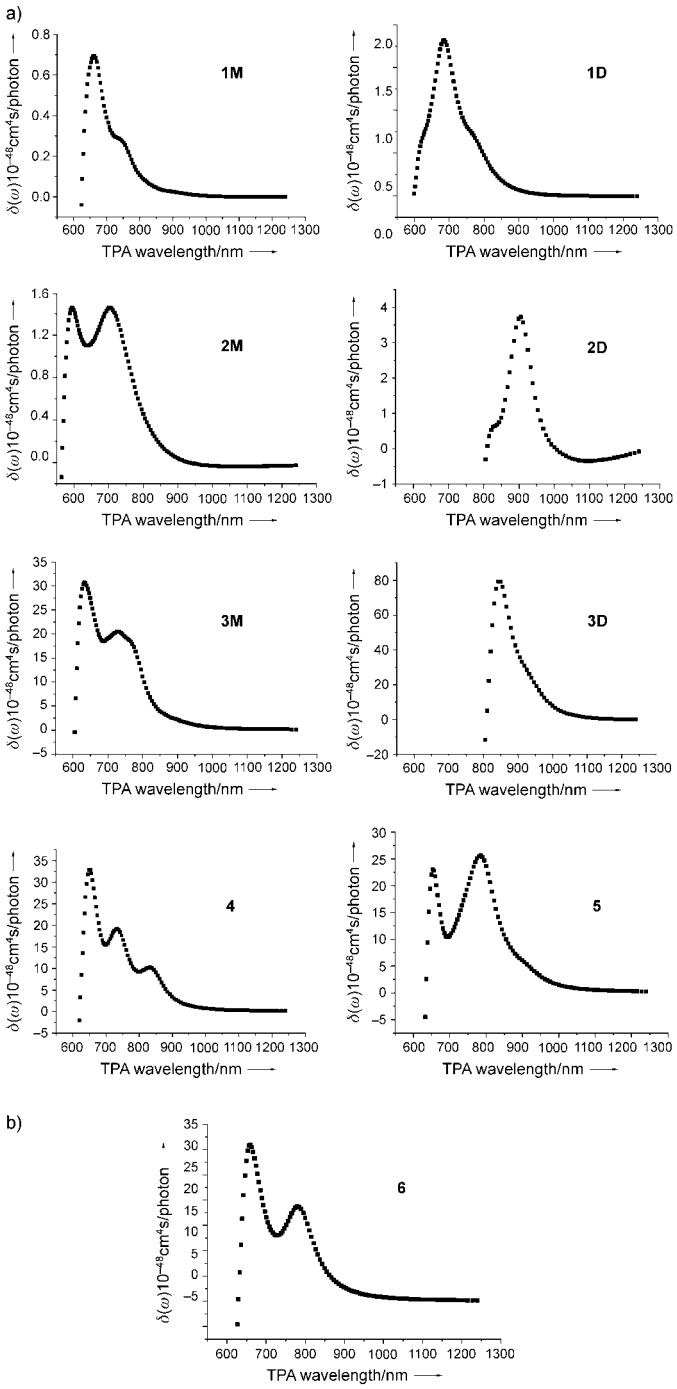

Figure 4. Two-photon absorption spectra.

peak at the longest wavelength in every TPA spectrum (shown in boldface). The calculated TPA maximum $\lambda_{max}^{(2)}$ is observed at 663.0 nm for **1M**, and undergoes a red shift as the conjugation length is increased to **2M** (704.4 nm) and further to **3M** (729.3 nm). A similar red-shift in maximum TPA wavelength is observed when processing from **1D** (685.0 nm) to **2D** (905.0 nm) and to **3D** (849.2 nm).

As displayed in Table 1, from **1M** to **2M**, the maximum TPA cross section produces more than twofold enhancement from 0.69×10^{-48} to 1.45×10^{-48} cm^{4}s per photon. The introduction of a butadiyne moiety in **3M** increases the TPA cross section of **2M** by more than one order of magnitude (14 times). The similar trend is observed in dimer porphyrins (1.82×10^{-48} (**1D**), 3.72×10^{-48} (**2D**), 79.35×10^{-48} cm^{4}s per photon (**3D**)). The maximum TPA cross section of **3D** is about 21 times that of **2D**, due to the introduction of butadiyne linkages. These results indicate that the effect of the expansion of the π conjugation between porphyrin moieties by introducing a butadiyne linkage on the TPA cross section is essentially significant. The TPA cross section values of dimers **1D**, **2D**, and **3D** are twice to three times those of the corresponding monomers **1M**, **2M**, and **3M**, respectively. As can be seen from Table 1, the TPA cross section of compound **5** is larger than that of **3M** by 20%. The results above suggest that the complementary coordination of Zn atom has a positive effect on the enhancement in TPA cross section. Inspecting the TPA properties of molecules **4**, **5**, and **6**, we find that compound **5** exhibits the largest TPA cross section (25.61×10^{-48} cm^{4}s per photon), which is about 2.5 times as that of **4** and 36% larger than that of molecule **6**. The terminal free base, working as a primary electron acceptor in a photosynthetic reaction center, is certainly regarded as the acceptor with respect to the inner zinc por-

phyrin. From the frontier orbitals of molecule **5** in Figure 2, the charge transfer from the donor (zinc porphyrin) to the acceptor (free-base porphyrin) is clearly observed. The intramolecular charge transfer favors the enhancement of TPA cross section. These clearly show that, the increase of polarization by mono-metalation due to the combination of terminal free base and the core zinc porphyrin is another effective factor for increasing the TPA cross section.

Conclusion

In this paper, the molecular geometries, electronic structures, and one- and two-photon absorption properties of a series of self-assembled porphyrin derivatives have been investigated theoretically. Our calculations show that the introduction of butadiyne linkages and the increase of molecular dimensionality from monomer to dimer determine the OPA intensities of the Q-band and B-band absorptions, respectively. Introducing a butadiyne linkage is the overriding factor to increase the TPA cross-section value. The complementary coordination from monomers to dimers and introduction of electron-acceptor groups are also two effective factors for the enhancement of the TPA efficiency. The porphyrin analogues with the similar structures to **3D** would be a promising direction for further development of novel TPA materials.

Acknowledgement

This work is supported by the National Nature Science Foundation of China (20273023), the University Doctoral Subject Foundation of China, and the Key Laboratory for Supramolecular Structure and Material of Jilin University.

[1] C. Halvorson, A. Hays, B. Kraabel, R. Wu, F. Wudl, A. J. Heeger, *Science* **1994**, *265*, 1215.
[2] S. Maruo, O. Nakamura, S. Kawata, *Opt. Lett.* **1997**, *22*, 132.
[3] B. H. Cumpston, S. P. Ananthavel, S. Barlow, D. L. Dyer, J. E. Ehrlich, L. L. Erskine, A. A. J. Qin, H. Röckel, M. Rumi, X. L. Wu, S. R. Marder, J. W. Perry, *Nature* **1999**, *398*, 51.
[4] S. Kawata, H.-B. Sun, T. Tanaka, K. Takada, *Nature* **2001**, *412*, 697.
[5] S. Maruo, K. Ikuta, *Proc. SPIE-Int. Soc. Opt. Eng.* **2000**, *3937*, 106.
[6] H. E. Pudavar, M. P. Joshi, P. N. Prasad, B. A. Reinhardt, *Appl. Phys. Lett.* **1999**, *74*, 1338.
[7] W. Denk, *Proc. Natl. Acad. Sci. USA* **1994**, *91*, 6629.
[8] R. M. Williams, D. W. Piston, W. W. Webb, *FASEB J.* **1994**, *8*, 804.
[9] G. Chen, S. Mukamel, *J. Phys. Chem.* **1996**, *100*, 11080.
[10] R. R. Tykwinski, U. Gubler, R. E. Martin, F. Diederich, C. Bosshard, P. Günter, *J. Phys. Chem. B* **1998**, *102*, 4451.
[11] S. Hahn, S. Kim, M. Cho, *J. Phys. Chem. B* **1999**, *103*, 8221.
[12] M. Terazima, H. Shimizu, A. Osuka, *J. Appl. Phys.* **1997**, *81*, 2946.
[13] J. R. G. Thorne, S. M. Kuebler, R. G. Denning, I. M. Blake, P. N. Taylor, H. L. Anderson, *Chem. Phys.* **1999**, *248*, 181.
[14] S. M. Kuebler, R. G. Denning, H. L. Anderson, *J. Am. Chem. Soc.* **2000**, *122*, 339.
[15] M. Albota, D. Beljonne, J. L. Brédas, J. E. Ehrlich, J. Fu, A. A. Heikal, E. Hess, T. Kogej, M. D. Levin, S. R. Marder, D. McCord-Maughon, J. W. Perry, H. Röeckel, M. Rumi, G. Subramaniam, W. W. Webb, X. Wu, C. Xu, *Science* **1998**, *281*, 1653.
[16] O.-K. Kim, K.-S. Lee, H. Y. Woo, K.-S. Kim, G. S. He, J. Swiatkiewicz, P. N. Prasad, *Chem. Mater.* **2000**, *12*, 284.
[17] B. R. Cho, K. H. Son, S. H. Lee, Y.-S. Song, Y.-K. Lee, S.-J. Jeon, J.-H. Choi, H. Lee, M. Cho, *J. Am. Chem. Soc.* **2001**, *123*, 10039.
[18] D. Beljonne, W. Wenseleers, E. Zojer, Z. Shuai, H. Vogel, S. J. K. Pond, J. W. Perry, S. R. Marder, J.-L. Brédas, *Adv. Funct. Mater.* **2002**, *12*, 631.
[19] M. Drobizhev, A. Karotki, Y. Dzenis, A. Rebane, Z. Suo, C. W. Spangler, *J. Phys. Chem. B* **2003**, *107*, 7540.
[20] L. Porrès, O. Mongin, C. Katan, M. Charlot, T. Pons, J. Mertz, M. Blanchard-Desce, *Org. Lett.* **2004**, *6*, 47.
[21] R. Kannan, G. S. He, T.-C. Lin, P. N. Prasad, R. A. Vaia, L.-S. Tan, *Chem. Mater.* **2004**, *16*, 185.
[22] T. C. Wen, L. C. Hwang, W. Y. Lin, C. H. Chen, C. H. Wu, *Chem. Phys.* **2003**, *286*, 293.
[23] A. Karotki, M. Drobizhev, M. Kruk, C. Spangler, E. Nickel, N. Mamardasvili, A. Rebane, *J. Opt. Soc. Am. B* **2003**, *20*, 321.
[24] T. E. O. Screen, J. R. G. Thome, R. G. Denning, D. G. Bucknall, H. L. Anderson, *J. Am. Chem. Soc.* **2002**, *124*, 9712.
[25] A. Karotiki, M. Drobizhev, Y. Dzenis, P. N. Taylor, H. L. Anderson, A. Rebane, *Phys. Chem. Chem. Phys.* **2004**, *6*, 7.
[26] M. B. Masthay, L. A. Findsen, B. M. Pierce, D. F. Bocian, J. S. Lindsey, R. B. Birge, *J. Chem. Phys.* **1986**, *84*, 3901.
[27] X. Zhou, A.-M. Ren, J.-K. Feng, X.-J. Liu, *ChemPhysChem* **2003**, *4*, 991.
[28] K. Ogawa, A. Ohashi, Y. Kobuke, K. Kamada, K. Ohta, *J. Am. Chem. Soc.* **2003**, *125*, 13356.
[29] M. Cha, W. E. Torruellas, G. I. Stegeman, W. H. G. Horsthuis, G. R. Möhlmann, J. Meth, *Appl. Phys. Lett.* **1994**, *65*, 2648.
[30] T. Kogej, D. Beljoone, F. Meyers, J. W. Perry, S. R. Marder, J.-L. Brédas, *Chem. Phys. Lett.* **1998**, *298*, 1.
[31] B. J. Orr, J. F. Ward, *Mol. Phys.* **1971**, *20*, 513.
[32] D. M. Bishop, J. M. Luis, B. Kirtman, *J. Chem. Phys.* **2002**, *116*, 9729.
[33] Y. Kobuke, K. Ogawa, *Bull. Chem. Soc. Jpn.* **2003**, *76*, 689.
[34] M. Gouterman, *J. Chem. Phys.* **1960**, *33*, 1523.
[35] M. Gouterman, in *Porphyrins, Vol. III* (Ed: D. Dolphin) Academic Press, New York, **1978**, p. 1.
[36] K. A. Nguyen, R. Pachter, *J. Chem. Phys.* **2001**, *114*, 10757.
[37] M. Rumi, J. E. Ehrlich, A. A. Heikal, J. W. Perry, S. Barlow, Z. Hu, D. McCord-Maughon, T. C. Parker, H. Röckel, S. Thayumanavan, S. R. Marder, D. Beljonne, J.-L. Brédas, *J. Am. Chem. Soc.* **2000**, *122*, 9500.
[38] K. Ogawa, T. Zhang, K. Yoshihara, Y. Kobuke, *J. Am. Chem. Soc.* **2002**, *124*, 22.
[39] B. A. Reinhardt, L. L. Brott, S. J. Clarson, A. G. Dillard, J. C. Bhatt, R. Kannan, L. Yuan, G. S. He, P. N. Prasad, *Chem. Mater.* **1998**, *10*, 1863.
[40] O.-K. Kim, K.-S. Lee, H. Y. Woo, K.-S. Kim, G. S. He, J. Swiatkiewicz, P. N. Prasad, *Chem. Mater.* **2000**, *12*, 284.

Received: March 16, 2004
Revised: June 25, 2004
Published online: October 7, 2004

